This is the accepted manuscript. For the published article, see:

Anderson, M., Gebbie-Rayet, J., Hill, A. *et al.* Predicting crystal growth via a unified kinetic three-dimensional partition model. *Nature* **544,** 456–459 (2017). https://doi.org/10.1038/nature21684

Predicting crystal growth via a unified kinetic three-dimensional partition model

Michael W. Anderson[1], James T. Gebbie-Rayet[1†], Adam R. Hill[1], Nani Farida[1], Martin P. Attfield[1], Pablo Cubillas[1†], Vladislav A. Blatov[2,3], Davide M. Proserpio[2,4], Duncan Akporiaye[5], Bjørnar Arstad[5] & Julian D. Gale[6]

[1]Centre for Nanoporous Materials, School of Chemistry, The University of Manchester, Oxford Road, Manchester M13 9PL, UK.
[2]Samara Center for Theoretical Materials Science (SCTMS),
Samara University, Academician Pavlov Street 1, Samara 443011, Russia.
[3]School of Materials Science and Engineering, Northwestern Polytechnical University, Xi'an, Shaanxi 710072, China.
[4]Università degli Studi di Milano, Dipartimento di Chimica, Via Camillo Golgi 19, 20133 Milano, Italy.
[5]SINTEF Materials and Chemistry, PO Box 124, Blindern, 0314 Oslo, Norway.
[6]Curtin Institute for Computation, Department of Chemistry, Curtin University, GPO Box U1987, Perth, Western Australia 6845, Australia.
†Present addresses: Scientific Computing Department, STFC Daresbury Laboratory, Warrington WA4 4AD, UK (J.T.G.-R.); Earth Sciences Department, Durham University, Lower Mountjoy, South Road, Durham DH1 3LE, UK (P.C.).

Understanding and predicting crystal growth is fundamental to the control of functionality in modern materials. Despite investigations for more than one hundred years[1–5], it is only recently that the molecular intricacies of these processes have been revealed by scanning probe microscopy[6–8]. To organize and understand this large amount of new information, new rules for crystal growth need to be developed and tested. However, because of the complexity and variety of different crystal systems, attempts to understand crystal growth in detail have so far relied on developing models that are usually applicable to only one system[9–11]. Such models cannot be used to achieve the wide scope of understanding that is required to create a unified model across crystal types and crystal structures. Here we describe a general approach to understanding and, in theory, predicting the growth of a wide range of crystal types, including the incorporation of defect structures, by simultaneous molecular-scale simulation of crystal habit and surface topology using a unified kinetic three-dimensional partition model. This entails dividing the structure into 'natural tiles' or Voronoi polyhedra that are metastable and, consequently, temporally persistent. As such, these units are then suitable for re-construction of the crystal via a Monte Carlo algorithm. We demonstrate our approach by predicting the crystal growth of a diverse set of crystal types, including zeolites, metal–organic frameworks, calcite, urea and l-cystine.

By understanding crystal growth at the molecular scale it is possible to control crystal habit, crystal size, the elimination or incorporation of defects and the development of intergrowth structures. Because crystals are used, for example, in technologies including pharmaceuticals and gas storage, as separation materials, in optoelectronic devices and as heterogeneous catalysts, such understanding is vital. We can illustrate many of the problems that must be addressed in crystal growth by considering zeolites[12] as an example, which represent a very complex, yet important, crystal type that forms the backbone of the heterogeneous catalysis industry. Zeolites are nanoporous materials for which the framework of the material is constructed from a strong, covalently bonded network of Si–O and Al–O bonds. The pores of the material are filled with water and cations that balance the negative charge on the framework. Crystals of zeolites grow from aqueous solutions at temperatures up to about 230 °C and it is well known from nuclear magnetic resonance spectroscopy that the solution phase exhibits very complex speciation[13–16]. This is a seemingly intractable problem in terms of defining a simple set of rules that govern the hundreds of different zeolite structures, let alone the thousands of related crystal structures such as metal–organic frameworks (MOFs)[17–19]. However, the course of a crystallization is relatively predictable and, therefore, there must be a relatively small number of rules that govern the most important aspects of the crystal growth, with subsidiary rules governing deviations.

The starting point in our simplification comes from a general Monte Carlo simulation applied to the growth of fats[20]. In this work it was shown that the principal determinant of crystal growth was the local internal energy at the crystal surface in relation to the chemical potential of the phase from which the crystal grows. This is a very important simplification because it allows the growth medium—solution, melt, gas and so on—to be considered to have only a growth potential, and so the speciation does not need to be considered in detail. Although this growth potential will be a result of the speciation, this can be treated as a subsidiary effect to be considered subsequently[13–16]. In the case of multicomponent crystals—such as MOFs or co-crystals for which species in solution, for example, linkers and metal centres, cannot interchange— a driving force for each component needs to be considered, unless the stoichiometries of the two phases are matched. For zeolites, or any system in which the nutrient is interconverting, a single driving force can be considered equivalent to a

single-component system. The crystal structure then needs to be broken down into 'units of growth', a process that is normally referred to as 'coarse-graining the problem'. To deconstruct the problem, we require a distinction between 'unit of growth' and 'growth unit'. To identify a growth unit, we need to know the growth mechanism, however, a unit of growth is just a suitable division of the structure in terms of metastability. If the material of interest is a molecular crystal, then a unit of growth would be a single molecule, because this represents a strongly bonded entity that remains intact during crystallization, forming relatively weak bonding with neighbours to yield the crystal. Such a unit of growth is probably, in many cases, the actual growth unit for the crystal, assuming that the unit does not dimerize in solution. However, for a zeolite, which is a fully connected three-dimensional network of covalent bonds, a single-molecule unit of growth is not viable. For our analysis, the unit of growth is any structural element that represents a metastable surface structure with small enough dimensions to describe all of the intricacies of the crystal formation. As a metastable entity it will be persistent in time at the crystal surface during growth and can therefore be considered to determine the overall rate of crystal growth. For the simulation of the full three-dimensional growth of a crystal, for example via the development of a kinetic Monte Carlo model, only the rate-determining steps are required. We now return to the problem of nanoporous zeolites composed of condensed tetrahedral silicate units forming cage-like structures. These cages are strongly related to metastable surface entities because the cage wrapping permits maximum condensation of the cage[11]. Consider a cage within the bulk of the zeolite with all tetrahedral silicon sites fully condensed (termed Q_4 units). When the same cage is located at the surface of the zeolite crystal, most of the silicon sites will lose only one bond of condensation, making this structural configuration a minimum in energy for a surface moiety. Of the more than 200 zeolite structures, around one quarter consist of Q_4 units that will lose only one condensation at the surface ($Q_4 \rightarrow Q_3$). The other three quarters have Q_4 units that may lose two condensations ($Q_4 \rightarrow Q_2$); however, these structures will still be at an energy minimum. Therefore, the cages become a suitable unit of growth even though they are not the growth unit. These cages are three-dimensional space-filling tiles that can be computed in a relatively straightforward manner using algorithms such as those implemented in ToposPro[21,22] (Fig. 1). Consequently, this establishes a simplified route to coarse-graining the zeolite problem into energetically minimized, metastable, rate-determining steps that, when balanced against a potential energy driving force from the growth medium, permits generation of a general kinetic Monte Carlo algorithm for zeolites. We use the so-called 'natural tiles' that describe the system of minimal cages in a unique and unambiguous way according to a strict algorithm[21]. In this regard it is very different to the diverse systems of secondary building units often chosen by structural chemists according to their personal view on how to divide up structures. The units of growth are space-filling and, although the crystal is nanoporous, they are considered to fill all space during growth (the voids within cages are filled with water and cations). This property is the same for the growth of any crystal, whether nanoporous or not.

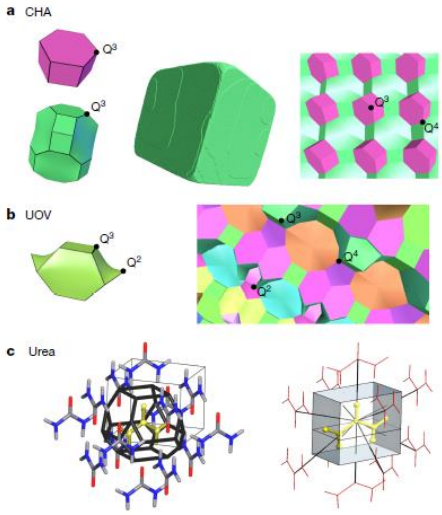

Figure 1 | Demonstration of the tiling and Voronoi-polyhedra partitioning methods. a, The chabazite structure (CHA), which is composed of two cages (tiles), the double 6-ring (pink) and chabazite cage (green). Both of these tiles consist entirely of Q_3 tetrahedra and are considered as closed cages or tiles. As the crystal grows (middle), the cages condense and the Q_3 vertices are converted into Q_4 vertices (right), thereby stabilizing the cage relative to the solution phase. **b**, The complex UOV structure, which consists of 16 tiles (see Extended Data Fig. 3). One of these tiles is shown, one that consists of both Q_3 and Q_2 vertices and is therefore considered as an open cage or tile (see Methods for definition of open versus closed cages and tiles). Condensation again results in stabilization of these tiles relative to the solution phase. **c**, A tile representation of the molecular crystal urea. The left panel shows the initial Voronoi construction with 14 urea neighbours surrounding the central molecule. Four of these interactions are very weak and can be neglected, leaving the ten interactions represented by the black lines in the right panel. Each interaction passes through the face of the ten-sided tile. Grey, red and blue represent carbon, oxygen and nitrogen atoms, respectively, the yellow represents the central urea molecule, and the black edges illustrate the Voronoi polyhedron created by these molecular interactions.

Our approach is extendable to any cage-like structure, regardless of the bonding type, so MOFs with extensive coordination bonds are immediately treatable. To extend our approach to other crystals we use the Voronoi partitioning procedure to fill the space with polyhedral units, in a manner opposite to that used for the tiling method: with Voronoi polyhedra, the objects (atoms or molecules) occupy the centres, whereas with tiles they occupy vertices. Molecular crystals, such as aspirin, urea and water, can be categorized as a three-dimensional Voronoi partition, in which the molecule sits at the centre of a Voronoi polyhedron and the faces of the polyhedron represent the interactions with neighbouring molecules (Fig. 1). Similarly, for ionic crystals, such as calcite and zinc oxide, the ions sit at the centres of Voronoi polyhedra with faces representing the interactions between cations and anions. In these last two examples, the network of interactions can be considered without needing to introduce three-dimensional partitioning; however, it is useful to realize that all crystal systems can be treated in the same manner. To summarize, we assume the units of growth to be polyhedral (tiles or Voronoi polyhedra depending on nature of the crystal). The Voronoi partition can also be used for structures that have no tiling, for example, for polycatenated networks. Having partitioned the crystal space, the problem then is to establish the energies of all of the three-dimensional polyhedral units in any configurationand the degree of condensation/attachment at the surface of a growing crystal relative to the bulk phase. For complex crystal systems there could be thousands of possible types of surface site, although, in principle, only a fraction of these will be topologically viable during crystal growth. By interfacing our kinetic Monte Carlo code with the three-dimensional partitioning approach of ToposPro22, we can compute all of the possible connectivities for any partitioning pattern and, consequently, any crystal structure. Then, to a first approximation, the energies of the polyhedral units are directly related to the degree of condensation or attachment (see Extended Data Fig. 1 for the LTA zeolite system). Secondary energetic effects can be computed at a much higher level of simulation to determine subsidiary effects, but most structural features are determined purely by connectivity. Common defects, such as screw dislocations, can be incorporated by displacing three-dimensional polyhedral units to equivalent sites along the screw core, resulting in perfect crystal re-connection. Growth modifiers can also be simulated by poisoning units of growth accordingly (that is, by reducing their probability of growth). This approach permits both growth and dissolution at individual surface sites, depending on whether the chemical potential of the growth medium is above or below the energy of that surface site. In this manner, by changing the driving force systematically within the simulation, the equilibrium morphology is found when the rates of growth and dissolution are balanced. Examples for the LTA and FAU zeolite structures are shown in Extended Data Figs 1 and 2, respectively, illustrating how both the habit of the crystal and the much more sensitive surface topology can be matched with experiment across all crystal faces. This approach enables straightforward computation of crystals no matter what degree of complexity exists in the structure; for example, the UOV zeolite structure (Fig. 2 and Extended Data Fig. 3), which has a very large unit cell and is constructed from 16 tiles in a mixture of open and closed environments, is readily treated in an efficient manner. For such a system, even using the same energy penalty for every tile vertex gives both a crystal habit and surface topology very similar to that observed experimentally. This computation yields the terrace structure, which also includes the nature of the surface termination that, for nanoporous materials, is the gateway to the internal porosity. This approach also demonstrates how framework crystals such as NES (Extended Data Fig. 4) have great difficulty circumventing large cages that will necessarily represent large energy barriers. The resulting crystals are very thin plates and any modification to this morphology would require careful attention to the stabilizing of the large cage through templating.

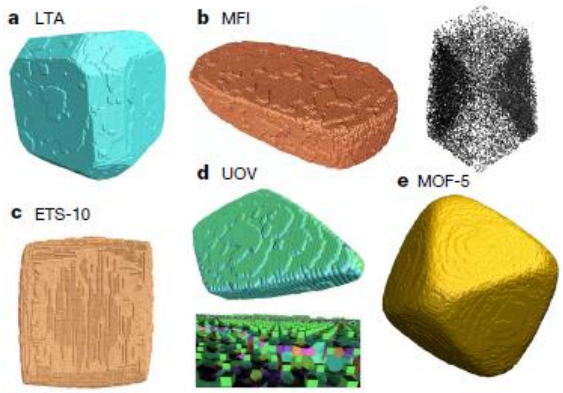

Figure 2 | Results of simulations run on various framework types. **a**, LTA (zeolite A) consists of three closed cages (tiles), and the experimental morphology can be achieved by adjusting the energy of these tiles independently relative to solution (see Extended Data Fig. 1 and Supplementary Video 1). **b**, MFI (also known as ZSM-5 or silicalite) is a complex structure consisting of 10, all open, tiles. The morphology and topology can be simulated very well using different energy penalties for large and small tiles. Interrogation of the internal structure of the crystal reveals an hourglass structure similar to that observed experimentally by optical microscopy. This structure is due to crystallization with incomplete condensation of tiles resulting in the silanol groups that are known to be present in the ZSM-5 structure (see Extended Data Fig. 5 and Supplementary Video 4). **c**, ETS-10 is a mixed-coordination octahedral and tetrahedral nanoporous framework structure that consists of titanate rods that are stacked layer by layer in an orthogonal arrangement. Viewed down the [001] axis, as is the case here, the rod-based crystal growth mechanism is immediately apparent; such a growth mechanism leads to the incorporation of defects (see Extended Data Fig. 6 and Supplementary Video 5). **d**, UOV is one of the most complex zeolite structures, with a very large unit cell and 16, both open and closed, tiles. Our methodology is able to efficiently grow such a complex structure with both surface topography and habit matching experimental observations. The surface structure (top) is determined from the calculations, as is the nature of partially constructed layers (bottom) at intermediate metastable steps (see Extended Data Fig. 3 and Supplementary Video 3). **e**, MOFs can be modelled using two differing methods: first, by treating them as multicomponent molecular crystals, with metal clusters and organic linkers treated as separate molecules (as in MOF-5); and second, by using the same treatment as zeolite frameworks (as seen with HKUST-1 in Extended Data Fig. 9a–d and Supplementary Video 6). Again the crystal habit and surface topography match those observed experimentally with different crystallization conditions (further examples are shown for MOF-5 in Extended Data Fig. 9e–i).

The MFI zeolite framework type, also known as ZSM-5—one of the most important industrial catalysts—reveals not only the surface structure but also the internal structure of the crystals. Within the bulk of the crystal, tiles remain incomplete in other words, they possess dangling silanol groups—consistent with the many internal silanols that are well-established to be present in ZSM-5. The interesting discovery is that, because the growth mechanisms on different faces of the crystal are necessarily different, the silanols are confined to zones of different density within the crystal (Fig. 2 and Extended Data Fig. 5). This finding mimics almost exactly the optical birefringence, showing zoning identical to that observed experimentally (Extended Data Fig. 5) and has been a source of debate for many years[23].

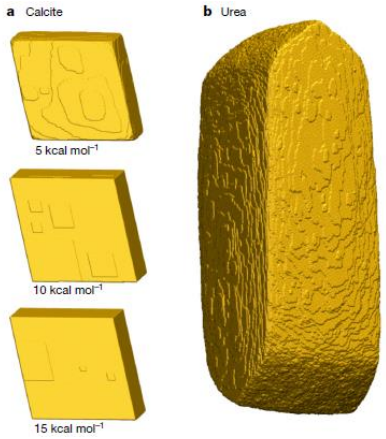

Figure 3 | Simulations of an ionic crystal (calcite) and a molecular crystal (urea). a, **b**, Simulations of calcite (**a**) and urea (**b**), demonstrating the universality of our approach to different crystal classes. All simulations are shown under equilibrium conditions. **a**, For calcite, the reaction energy for the conversion of solubilized ions to the crystal per coordination to the crystal is set at 5 kcal mol^{-1}, 10 kcal mol^{-1} or 15 kcal mol^{-1}. Calculations show that the value lies between 10 kcal mol^{-1} and 15 kcal mol^{-1}, and the crystal habit and surface topography of the two corresponding simulations match experiment closely. At 5 kcal mol^{-1}, the terrace edges are much more rounded than observed experimentally. The main difference between the simulations for 10 kcal mol^{-1} and 15 kcal mol^{-1} is the terrace density, which can also be used as a distinguishing factor. **b**, For urea, three different reaction energies are used, depending primarily on the strength of interaction in the urea crystal (discussed in Methods). The large {110} faces are flat and dominated by terraces elongated in the *c* direction of the crystal (vertical in the image). The smaller pseudo-{111} faces are rough and generated in a large part by dissolution when the supersaturation is close to equilibrium.

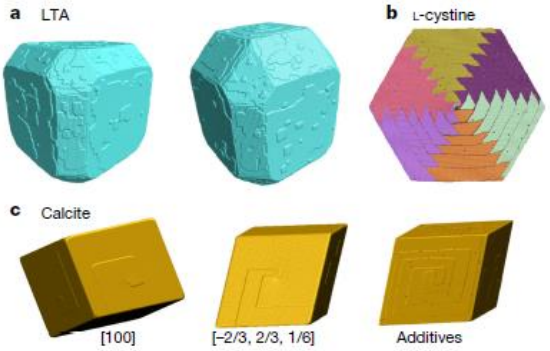

Figure 4 | Results of incorporating screw dislocations in growing LTA, l-cystine and calcite crystals. Screw dislocations may be computed using our methodology for any crystal system along any crystal direction. This method operates according only to topology and does not account for the energy of the crystal at the screw core. Nonetheless, it allows all possible topologically permitted structures to be tested for growth morphology; energy considerations can be determined separately. **a**, Simulations of LTA structure with (right) and without (left) a screw dislocation running along [100] through the crystal, vertically. A lengthening of the crystal along the [100] direction is immediately apparent, owing to the greater ease for growth at the spiral growth front. This demonstrates how the relative growth rates of layer-by-layer growth versus spiral growth can be determined. **b**, Pin-wheel crystal growth formation in the l-cystine system caused by the 6_1 screw axis, with hexagonal terraces consisting of six individual l-cystine layers forming a step bunch circumscribed by the slow growth directions. Progression of the step bunches and of single steps is the result of a complex interplay between attachment at single step edges, step bunches and surface sites that can be seen in Supplementary Video 7. **c**, Screw dislocations in calcite. The left panel shows a single screw dislocation with screw core along [100]. Such a dislocation emanates on two adjacent {104} crystal faces. Calcite is also known to exhibit double screw dislocations and the middle panel shows a double Burgers vector screw along $[-2/3, 2/3, 1/6]$, which has the smallest displacement possible for such a double screw. The right panel shows the effect of selective 'poisoning' (via the addition of additives) at two-coordinate sites along terrace edges (red dots), which produces rounding of terrace features.

Similarly, in ETS-10, which displays rod growth (Extended Data Fig. 6) rather than layer growth, the incompleteness of the rods results in internal defects that congregate in a zone from the (001) facets to the centre of the crystal, as observed experimentally by Raman microscopy[24]. Our kinetic three-dimensional partitioning model shows that a straightforward growth mechanism can explain these optical phenomena without the need for complex arguments related to twinning of the crystals. Common defect structures, such as

screw dislocations, are able not only to replicate the spiral topology, such as in LTA and CHA (Extended Data Figs 1 and 7, respectively), but also indicate the relative growth rates of the screw in relation to the layer growth. Complex interleaving of screw formation owing to fast and slow growth directions, such as seen in the AEI zeolite system (Extended Data Fig. 8), can be faithfully reproduced. Also, the direction of the screw core can be interrogated according to the multiplicity of the spiral growth emanating at the crystal surface, such as in the metal–organic HKUST-1 (Extended Data Fig. 9a–d). Indeed, MOFs are as readily treated as zeolites using this approach, either as cage (partitioned) structures as in HKUST-1 or as molecular crystals as shown for MOF-5 (Extended Data Fig. 9e–i). In the latter case, it is necessary also to consider the solvent as an important element in the crystal growth, because without it the observed crystal habit and surface topology cannot be replicated. MOF-5 is a good example of a multicomponent crystal, demonstrating the power of our approach to this important general class of materials. Molecular crystals and ionic crystals (Figs 3 and 4, respectively) are both amenable to this treatment and, for calcite, the crystallization energies are in broad agreement with those calculated using a combination of interatomic potentials and a continuum solvent model (see Methods). For the l-cystine system, it has been shown[25,26] that growth on the 〈001〉 face proceeds predominantly via screw dislocations. When this growth mechanism is augmented with the 6_1 screw axis of the crystal structure and with highly anisotropic rates of crystal growth, a complex pin-wheel surface topology is generated. Our simulations, which are based on four independent interaction energies, faithfully reproduce all of these growth features and reveal the importance of the interplay between different growth modes in the complete crystallization mechanism (Fig. 4 and Extended Data Fig. 10). Finally, the addition of growth modifiers is also readily achieved (Fig. 4), and was used to examine the targeting of specific growth sites in relation to the effect of these sites on the growth topology, yielding similar results to those observed experimentally[27]. The power of this approach is in the general applicability across crystal systems, and it provides a window of understanding that can be explored through higher-level calculations on each individual system.

Online Content Methods, along with any additional Extended Data display items and Source Data, are available in the online version of the paper; references unique to these sections appear only in the online paper.
Received 5 October 2016; accepted 1 February 2017.
Published online 3 April 2017.

1. Ostwald, W. Studien über die Bildung und Umwandlung fester Körper. *Z. Phys. Chem*. **22,** 289–330 (1897).
2. Volmer, M. *Kinetics of Phase Formation (Kinetik der Phasenbildung)* http://www.dtic.mil/cgi-bin/GetTRDoc?Location= U2&doc= GetTRDoc.pdf&AD= ADA800534 (Theodor Steinkopf, 1939).
3. Stranski, I. N. Zur Theorie des Kristallwachstums. *Z. Phys. Chem*. **136,** 259–278 (1928).
4. Kossel, W. Zur Theorie des Kristallwachstums. *Nachrichten der Gesselschaft der Wissenschaften Göttingen, Mathematisch-Physikalische Klasse* **1927,** 135–143, (1927).
5. Burton, W. K., Cabrera, N. & Frank, F. C. The growth of crystals and the equilibrium structure of their surfaces. *Phil. Trans. R. Soc. Lond. A* **243,** 299–358 (1951).
6. Hillner, P. E., Gratz, A. J., Manne, S. & Hansma, P. K. Atomic-scale imaging of calcite growth in real-time. *Geology* **20,** 359–362 (1992).
7. Land, T. A., DeYoreo, J. J. & Lee, J. D. An in-situ AFM investigation of canavalin crystallization kinetics. *Surf. Sci*. **384,** 136–155 (1997).
8. Agger, J. R., Pervaiz, N., Cheetham, A. K. & Anderson, M. W. Crystallization in zeolite A studied by atomic force microscopy. *J. Am. Chem. Soc.* **120,** 10754–10759 (1998).
9. Cuppen, H. M., van Veenendaal, E., van Suchtelen, J., van Enckevort, W.J.P. & Vlieg, E. A Monte Carlo study of dislocation growth and etching of crystals. *J. Cryst. Growth* **219,** 165–175 (2000).
10. De Yoreo, J. J. *et al.* Rethinking classical crystal growth models through molecular scale insights: consequences of kink-limited kinetics. *Cryst. Growth Des*. **9,** 5135–5144 (2009).
11. Brent, R. *et al.* Unstitching the nanoscopic mystery of zeolite crystal formation. *J. Am. Chem. Soc.* **132,** 13858–13868 (2010).
12. Davis, M. E. Ordered porous materials for emerging applications. *Nature* **417,** 813–821 (2002).
13. Kinrade, S. D. & Swaddle, T. W. ^{29}Si NMR studies of aqueous silicate solutions 2: transverse ^{29}Si relaxation and the kinetics and mechanism of silicate polymerisation. *Inorg. Chem*. **27,** 4259–4264 (1988).
14. Knight, C. T. G. & Harris, R. K. Silicon-29 nuclear magnetic resonance studies of aqueous silicate solutions 8: spin-lattice relaxation times and mechanisms. *Magn. Reson. Chem*. **24,** 872–874 (1986).
15. Harris, R. K. & Kimber, B. J. Si NMR as a tool for studying silicones. *Appl.Spectrosc. Rev*. **10,** 117–137 (1975).
16. Petry, D. P. *et al.* Connectivity analysis of the clear sol precursor of silicalite: are nanoparticles aggregated oligomers or silica particles? *J. Phys. Chem. C* **113,** 20827–20836 (2009).
17. Yaghi, O. M. *et al.* Reticular synthesis and the design of new materials. *Nature* **423,** 705–714 (2003).
18. Férey, G. Hybrid porous solids: past, present, future. *Chem. Soc. Rev.* **37,** 191–214 (2008).
19. Kitagawa, S., Kitaura, R. & Noro, S. Functional porous coordination polymers. *Angew. Chem. Int. Ed*. **43,** 2334–2375 (2004).
20. Boerrigter, S. X. M. *et al.* MONTY: Monte Carlo crystal growth on any crystal structure in any crystallographic orientation; application to fats. *J. Phys. Chem. A* **108,** 5894–5902 (2004).
21. Blatov, V. A., Delgado-Friedrichs, O., O'Keeffe, M. & Proserpio, D. M. Three-periodic nets and tilings: natural tilings for nets. *Acta Crystallogr. A* **63,** 418–425 (2007).
22. Blatov, V. A., Shevchenko, A. P. & Proserpio, D. M. Applied topological analysis of crystal structures with the program package ToposPro. *Cryst. Growth Des*. **14,** 3576–3586 (2014).
23. Roeffaers, M. B. J. *et al.* Morphology of large ZSM-5 crystals unraveled by fluorescence microscopy. *J. Am. Chem. Soc.* **130,** 5763–5772 (2008).
24. Jeong, N. C., Lim, H., Cheong, H. & Yoon, K. B. Distribution pattern of length, length uniformity, and density of TiO_{32-} quantum wires in an ETS-10 crystal revealed by laser-scanning confocal polarized micro-Raman spectroscopy. *Angew. Chem. Int. Ed*. **50,** 8697–8701 (2011).
25. Shtukenberg, A. G. *et al.* Dislocation-actuated growth and inhibition of hexagonal l-cystine crystallization at the molecular level. *Cryst. Growth Des*. **15,** 921–934 (2015).
26. Rimer, J. D. *et al.* Crystal growth inhibitors for the prevention of l-cystine kidney stones through molecular design. *Science* **330,** 337–341 (2010).

27. Teng, H. H., Dove, P. M. & DeYoreo, J. J. Reversed calcite morphologies induced by microscopic growth kinetics: insight into biomineralisation. *Geochim. Cosmochim. Acta* **63,** 2507–2512 (1999).

Supplementary Information is available in the online version of the paper.

Acknowledgements V.A.B. is grateful to the Russian Science Foundation (Grant No. 16-13-10158) for support. The Research Council of Norway, through the project Catlife, 'Catalyst transformation and lifetimes by in-situ techniques and modelling', P#233848, is acknowledged for financial support. A.R.H. and J.T.G.-R. are grateful for part funding from EPSRC through CASE awards. J.D.G. thanks the Australian Research Council for support through the Discovery Programme, and the Pawsey Supercomputing Centre and National Computational Infrastructure for provision of computing resources. We also acknowledge the Leverhulme Trust and the Royal Society for financial support.

Author Contributions M.W.A. conceived ideas, wrote the *CrystalGrower* growth code and performed simulations, J.T.G.-R. wrote an early version of the growth and visualization code and performed simulations, A.R.H. wrote the *CrystalGrower* visualization code and performed simulations, N.F. and P.C. recorded AFM images, M.P.A. coordinated MOF work, V.A.B. modified the ToposPro code to interface with *CrystalGrower*, D.M.P. developed ideas to integrate tiling methodology, D.A. and B.A. funded A.R.H. and contributed to discussions about the mechanism of crystal growth, and J.D.G. computed energetics for the calcite and L-cystine systems. All authors contributed to writing the manuscript.

Author Information Reprints and permissions information is available at www.nature.com/reprints. The authors declare no competing financial interests. Readers are welcome to comment on the online version of the paper. Publisher's note: Springer Nature remains neutral with regard to jurisdictional claims in published maps and institutional affiliations. Correspondence and requests for materials should be addressed to M.W.A. (m.anderson@manchester.ac.uk).

Reviewer Information *Nature* thanks M. Deem, M. Tuckerman and the other anonymous reviewer(s) for their contribution to the peer review of this work.